Biochimica et Biophysica Acta 1833 (2013) 2996–3005

Contents lists available at ScienceDirect

Biochimica et Biophysica Acta

journal homepage: www.elsevier.com/locate/bbamcr

Knock-down of glutaminase 2 expression decreases glutathione, NADH, and sensitizes cervical cancer to ionizing radiation

Lisha Xiang [a,b,1], Ganfeng Xie [a,b,1], Chen Liu [b], Jie Zhou [a], Jianfang Chen [a], Songtao Yu [a], Jianjun Li [a,c], Xueli Pang [b], Hang Shi [d], Houjie Liang [a,b,c,*]

[a] Department of Oncology, Southwest Hospital, the Third Military Medical University, Chongqing 400038, PR China
[b] Radiation Oncology Center, Southwest Hospital, the Third Military Medical University, Chongqing 400038, PR China
[c] Southwest Cancer Center, Southwest Hospital, the Third Military Medical University, Chongqing 400038, PR China
[d] Department of Biology, Georgia State University, Atlanta, GA 30303, USA

ARTICLE INFO

Article history:
Received 17 April 2013
Received in revised form 17 July 2013
Accepted 5 August 2013
Available online 13 August 2013

Keywords:
Phosphate-activated mitochondrial glutaminase
Radioresistance
Cervical cancer
Glutathione

ABSTRACT

Phosphate-activated mitochondrial glutaminase (GLS2) is suggested to be linked with elevated glutamine metabolism. It plays an important role in catalyzing the hydrolysis of glutamine to glutamate. The present study was to investigate the potent effect of GLS2 on radioresistance of cervical carcinoma. GLS2 was examined in 144 cases of human cervical cancer specimens (58 radioresistant specimens, 86 radiosensitive specimens) and 15 adjacent normal cervical specimens with immunohistochemistry. HeLa cells were treated with a cumulative dose of 50 Gy X-rays, over 6 months, yielding the resistant sub-line HeLaR. The expressions of GLS2 were measured by Western blot. Radioresistance was tested by colony survival assay. Apoptosis was determined by flow cytometry. The levels of glutathione (GSH), reactive oxygen species (ROS), NAD^+/NADH ratio and $NADP^+$/NADPH ratio were detected by quantization assay kit. Xenografts were used to confirm the effect of GLS2 on radioresistance *in vivo*. The expressions of GLS2 were significantly enhanced in tumor tissues of radioresistant patients compared with that in radiosensitive patients. *In vitro*, the radioresistant cell line HeLaR exhibited significantly increased GLS2 levels than its parental cell line HeLa. GLS2 silenced radioresistant cell HeLaR shows substantially enhanced radiosensitivity with lower colony survival and higher apoptosis in response to radiation. *In vivo*, xenografts with GLS2 silenced HeLaR were more sensitive to radiation. At the molecular level, knock-down of GLS2 increased the intracellular ROS levels of HeLaR exposed to irradiation by decreasing the productions of antioxidant GSH, NADH and NADPH. GLS2 may have an important role in radioresistance in cervical cancer patients.

1. Introduction

Cervical cancer is one of the most common malignancies among women worldwide with a high incidence and mortality, especially in developing countries [1]. In 2008, approximately 530,000 new cases were diagnosed, with more than 274,000 women dying of the disease [2]. Radiation therapy is the most broadly used treatment modality in patients with cervical cancers particularly at an advanced stage or that cannot be cured surgically [3]. However, despite progress in radiation technology, local recurrence still occurs in a large proportion of patients following radiotherapy because of radioresistance. Based on clinical evidence, enhanced DNA repair mechanisms [4], hypoxia [5], intrinsic radioresistance [6] and cellular glutathione [7] are contributing factors to this resistance. In addition, a growing body of evidence supports the idea that glutamine metabolism may involve in protecting tumor cells from lethal ionizing radiation (IR), which have been recognized as another potential mechanism of resistance to radiotherapy [8,9]. Therefore, we hypothesize that radioresistance is due also, in part, to altered expression of glutaminase, and we found phosphate-activated mitochondrial glutaminase (GLS2), the key enzyme in conversion of glutamine to glutamate and is overexpressed in radioresistant tumor tissues compared with radiosensitive tumor tissues after radiotherapy in cervical cancer patients. Thus, to investigate whether glutaminase could be a regulator of radioresistance and its underlying mechanisms may lead to advances in the radiotherapy of human cervical cancers.

Glutamine (Gln) is one of the essential nutrients for cancer cells and is the most abundant free amino acid in humans. Glutaminase (GA) is the major enzyme that catalyzes the hydrolysis of glutamine to glutamate, which is in turn converted to alpha-ketoglutarate for further

* Corresponding author at: Department of Oncology, Radiation Oncology Center and Southwest Cancer Center, Southwest Hospital, Third Military Medical University, 30 Gaotanyan Street, Chongqing 400038, China. Tel.: +86 23 68754128; fax: +86 23 65425219.
E-mail address: lianghoujie@sina.com (H. Liang).
[1] These authors contributed equally to this work.

0167-4889/$ – see front matter © 2013 Elsevier B.V. All rights reserved.
http://dx.doi.org/10.1016/j.bbamcr.2013.08.003

metabolism in the tricarboxylic acid cycle (TCA) [10]. Mammals contain at least two genes that encode distinct isozymes of GA. GLS1 that encodes the "kidney-type" isozyme (KGA) is abundantly expressed in kidney, brain, intestine, immune system cells and in many transformed cells, with the exception of postnatal liver [11]. GLS2 encodes the "liver-type" isozyme (LGA) and was originally thought to be present only in adult liver tissue [12]. Recently, emerging evidences documenting the presence of GLS2 in brain, pancreas and breast cancer cells have appeared [13]. Our research group has found that the expression of GLS2 also occurs in human cervical cancer.

Mitochondrial GA is truly a key metabolic enzyme, hydrolyzing amino acid Gln that boosts the ability of cells to grow and proliferate. However, GA's influence in cell biology and cancer extends far beyond its use as a major hydrolase in glutamine metabolism [14]. A number of recent reports have highlighted these "non-metabolic" functions of GA in regulating tumor cell survival, proliferation [15], metastasis [16], signal transduction [17], and autophagy [18]. However, the role of GA in radioresistance has not previously been investigated. On the basis of the result that GLS2 is overexpressed in radioresistant cervical cancer tissues, we hypothesized that GLS2 may act as a pivotal factor in inducing radioresistance in cervical cancer. The aim of this study was to evaluate the hypothesis that GLS2 may cause radioresistance in cervical cancer. Thus, long-term X-ray irradiation of HeLa cells was used to generate the radioresistant cell sub-lines, HeLaR, and we found that GLS2 overexpression is required for sustaining radioresistance of HeLaR. Additionally we unveiled that silencing GLS2 expression caused down-regulation of cellular antioxidant glutathione, NADH and NADPH levels, and then, decreasing depletion of reactive oxygen species (ROS) and enhancing radiosensitivity of cervical cancer. Our finding for the first time links GLS2 to radioresistance-associated properties of cervical carcinomas.

2. Methods and materials

2.1. Ethics statement

Experiments using the animals were conducted with the approval of the Animal Care and Use Committee of Third Military Medical University (Approval ID: SCXK (Military) 2007015), according to the State Science and Technology Commission Regulations for the Administration of Affairs Concerning Experimental Animals (1988, China).

The clinical investigation was complied with the ethical standards laid down in the 1964 Declaration of Helsinki. The protocol of immunohistochemistry for patient tissues was approved by the Ethic Committee of the first Affiliated Hospital (Southwest Hospital), Third Military Medical University (Permit Number: 2012[13]), and all patients or family members involved have provided written informed consent.

2.2. Patients and specimens

Patients with locally advanced stage IIB-IVA cervical cancer, who had undergone radiotherapy in the Radiation Oncology Center at Southwest Hospital, Third Military Medical University between 2000 and 2008, were identified. The clinical stages of cervical cancer were defined according to International Federation of Gynecology and Obstetrics (FIGO). Patients' clinical information was collected and stored in a database. Fifty-eight of specimens were selected from patients with local recurrence or radiation failure after primary radiation therapy, and constituted the radioresistant group. Eighty-six age-matched control specimens were selected from patients who had no local recurrence for at least 3 years after radiation therapy, which constituted the radiosensitive group. Adjacent normal specimens were collected from 15 cervical cancer patients who underwent surgery in Southwest Hospital. The histomorphology of all specimens had been confirmed by the Department of Pathology, Southwest Hospital.

2.3. Cell lines and irradiation

All human cancer cell lines were obtained from the ATCC (Manassas, VA, USA) and cultured in RPMI 1640 medium (GIBCO) or Dulbecco's modified Eagle's medium (GIBCO) supplemented with 10% newborn calf serum (GIBCO), penicillin (100 U/ml), and streptomycin (0.1 mg/ml) (Beyotime Institute of Biotechnology, China). Cells were incubated in 5% CO_2 at 37 °C and passaged 2–3 times weekly. For X-ray treatment, cells were cultured in 75 cm^2 culture flasks until they reached approximately 75% confluence and then irradiated at 200 cGy/min, at room temperature, with a high energy linear accelerator (Varian, USA) operating at 6 MV. Immediately after irradiation, the culture medium was renewed and then the cells were returned to the incubator. When HeLa cells incubated to approximately 90% confluence, they were trypsinized, counted and passaged into new culture flasks. The cells were treated with 2 Gy again when they reached about 75% confluence. X-ray resistant sub-line (HeLaR) was generated by continuous sublethal irradiation for 6 months with a 2Gy radiation repeated 25 times to the total dose of 50 Gy. The parental cell line (HeLa) was trypsinized, counted and passaged under the same conditions without ionizing irradiation. To control for acute effects of IR, the radioresistant sub-line was cultured for over 1–2 months after the last irradiation before being used in the analyses.

2.4. Construction and preparation of lentivirus for RNAi of GLS2

shRNA-GLS2 (GTGGTCAAACTGCTTCAAGAT) was designed against GLS2 (accession number: NM_013267) and synthesized as follows: Forward: 5′- ccggGTGGTCAAACTGCTTCAAGATctcgagATCTTGAAGCAG TTTGACCACttttttg-3′, and Reverse: 5′- aattcaaaaaaGTGGTCAAACTGC TTCAAGATctcgagATCTTGAAGCAGTTTGACCAC-3′. These oligos were annealed and inserted downstream of the U6 promoter on the lentiviral vector pGCL-GFP (Neuron Biotech). A control vector containing non-silencing sequence (5′-TTCTCCGAACGTGTCACGT-3′) was supplied by Neuron Biotech Co., Ltd. (Shanghai, China).

Lentiviruses were generated by triple transfection of 80% confluent HEK293T cells with pGCL-GFP-shGLS2 plasmid, together with pHelper 1.0 and pHelper 2.0 helper plasmids (Neuron Biotech) using Lipofectamine 2000 (Invitrogen, Carlsbad, CA, USA).

Lentivirus was harvested at 48 h and 72 h post transfection, centrifuged to remove cell debris, and then filtered through a 0.45 μm cellulose acetate filter followed by ultracentrifugation. For lentivirus infection, HeLaR cells were grown to 70–80% confluence and infected with pGCL-GFP-shGLS2 lentivirus or control lentivirus, separately, at MOI of 50 (HeLaR). To determine the infection efficiency, cells expressing GFP protein were imaged using laser confocal scanning microscopy (Leica TSC-SP5, Germany) 4 days after infection. The GFP positive cells were purified with a FACSCalibur flow cytometer (BD Biosciences).

2.5. Tissue microarrays and immunohistochemistry (IHC)

All slides were prepared from stored pretreatment paraffin-embedded tissue blocks from the cervical cancer patients who underwent surgery in Southwest Hospital. Briefly, 86 radiosensitive cervical cancer specimens were made into tissue microarrays using the tissuearrayerTMA-1(Beecher Instruments, WA, USA) as described previously [19]. Fifty-eight radioresistant specimens and 15 adjacent normal cervical specimens were reprocessed into formalin-fixed paraffin-embedded tissue blocks again, and then cut into 4 μm-thickness sections. The tissue microarrays and tumor sections were routinely dewaxed in xylene, rinsed in graded ethanol, and finally rehydrated in double-distilled water. Endogenous peroxidase activity was blocked by incubation in 3% hydrogen peroxide methanol for 15 min. Antigen retrieval was accomplished by heating the slides in 1 mM EDTA solution (pH8.0). After washing in phosphate-buffered saline and exposure to 10% normal goat serum for 10 min to reduce nonspecific binding, the

slides were incubated overnight at 4 °C with a 1:100 dilution of rabbit anti-human GLS2 polyclonal antibody (Epitomics, Burlingame, CA). The tissue microarrays and sections were stained using the SP method according to the kit instructions. The instantaneous SP supersensitive kit (SP-9001) was provided by Beijing Zhongshan Jinqiao biotechnology Co., Ltd.

2.6. Criteria for assessing immunohistochemical results

For each slide, five random fields were selected for scoring and a mean score of each slide was calculated in final analysis. Positive staining was accessed using a five scoring system: 0 (no positive cells), 1 (<10% positive cells), 2 (10%–40% positive cells), 3 (40%–70% positive cells), and 4 (>70% positive cells). To achieve accuracy, the intensity of positive staining was also used in a four scoring system: 0 (negative staining), 1 (weak staining exhibited as light yellow), 2 (moderate staining exhibited as yellow brown), and 3 (strong staining exhibited as brown). Protein expression index = (intensity score) × (positive score). Slides were examined and scored independently by two histopathologists blinded to other pathological information.

2.7. Western blotting analysis

Cell extracts were prepared and Western blotting was performed according to the instruction of RIPA buffer (Biotek Corporation, Beijing, China). Cell lysates were collected by centrifugation at 12,000 rpm for 15 min at 4 °C, and then transferred to clean microcentrifuge tubes. Protein concentration was determined with Bradford reagent (Bio-Rad), and equal amounts of proteins (50 μg) were run on a 10% SDS–PAGE gel and blotted onto polyvinylidene fluoride membranes. After blocking for 2 h at room temperature with 5% non-fat-dry milk, membranes were incubated with anti-GLS2 rabbit polyclonal antibody (Epitomics; 1:500) and anti-actin antibodies (Santa Cruz Biotechnology) at 4 °C overnight, respectively. The secondary antibody was HRP-conjugated anti-IgG (Boster Biotechnology, Wuhan, China). Membranes were then incubated with SuperSignal West Femto Maximum Sensitivity Substrate (Pierce, Rockford, IL, USA) for 1 min and imaged using a Gel Doc XR system (Bio-Rad).

2.8. Clonogenic assay for radiosensitivity

The cells were seeded into 24-well culture dishes in triplicates (1000 cells to each well). Cells were allowed to form colonies during 1 week, and then cells were treated with 0, 2, 4, 6, 8, and 10 Gy of X-ray radiation. After 2 weeks, clones were fixed with methanol and stained with a 1% crystal violet (Beyotime Institute of Biotechnology, China) for 10 min. Stained clones that had more than 50 cells were counted and cloning efficiency calculated as: cloning efficiency = (clone number/total cell number)*100%. The cell survival fraction (SF) was determined. A cell survival curve was drafted using GraphPad Prism 5.0 software and the single-hit multi-target model $SF = 1\text{-}(1\text{-}e^{-D/D0})^N$, where SF is the survival fraction; D, the radiation dose; D_0, the mean death dose; and N, the extrapolated number. The triplicate experiments were done independently.

2.9. Flow cytometry analysis for apoptosis and cell cycle

All cells were treated with 6 Gy of X-ray radiation. At 48 h post-irradiation, the cells were harvested, washed twice with PBS and then stained with Annexin V-APC (Becton Dickinson, San Jose, CA) according to the manufacturer's protocol. Cell apoptosis analysis was carried out by flow cytometry (Becton Dickinson FACSCalibur).

For cell cycle analysis, HeLa and HeLaR cells were treated with 6 Gy of X-ray radiation. At 24 h post-irradiation, the cells were harvested, fixed with 70% ethanol, and then stored at 4 °C for 24 h. Cell cycle analysis was carried out by flow cytometry (Becton Dickinson FACSCalibur) at 488 nm.

2.10. Measurement of levels of ROS

Flow cytometry and confocal fluorescence imaging of dihydroethidium (DHE)-fluorescence were used to measure cellular ROS levels. Dihydroethidium was oxidized by superoxide to a novel product which binds to DNA enhancing intracellular fluorescence. About 3×10^5 cells were harvested, washed with serum-free RPMI culture medium and incubated with 5 μM DHE (Beyotime Institute of Biotechnology, China) at 37 °C for 30 min. Then the cells were harvested, washed and resuspended in serum-free RPMI culture medium. DHE-fluorescence was analyzed by flow cytometry (excitation wavelength 325 nm, and emission wavelength 610 nm). Mean fluorescence intensity (MFI) was calculated after correction for autofluorescence and fold change calculated relative to unirradiated control.

For confocal microscopy, cells were suspended in serum-free RPMI culture medium containing 5 μM DHE, and incubated at 37 °C for 30 min. Cells were slightly washed with PBS and imaging was conducted by a laser confocal scanning microscopy (Leica TSC-SP5, Germany).

2.11. Measurement of levels of glutathione and $NADP^+$/NADPH ratio

The total glutathione (GSH) and oxidative glutathione (GSSG) were determined by colorimetric microplate assay kits (Beyotime Institute of Biotechnology, China). After treatment, about 1×10^7 cells were collected and centrifuged at 10,000 ×*g* for 10 min at 4 °C. The cells were resuspended in 20 μl cell medium. Ten microliters of cells was mixed with 30 μl 5% metaphosphoric acid, then frozen and thawed twice using liquid nitrogen and 37 °C water. The samples were centrifuged and the supernatant was used for GSH and GSSG assays. The total GSH level was measured by the DTNB-GSSG recycling assay [20]. The GSSG level was quantified by the same method as for total GSH after the supernatant was treated with 1 mol/L 2-vinylpyridine solution to remove the reduced GSH. The amount of reduced GSH was obtained by subtracting the amount of GSSG from that of total GSH.

The $NADP^+$/NADPH ratio was determined by $NADP^+$/NADPH quantitation colorimetric kit (Biovision, USA). All cells were washed with PBS, scraped, and collected. After centrifugation, 10^6 cells in each group were resuspended in the $NADP^+$/NADPH extraction buffer included in the $NADP^+$/NADPH quantification kit. The $NADP^+$/NADPH ratio was determined following the manufacturer's protocol.

2.12. Measurement of intracellular pyridine nucleotides concentration

NADH and NAD^+ levels were measured by using the EnzyChrom™ NAD^+/NADH Assay Kit (BioAssay Systems, Hayward, CA) according to manufacturer's instructions. This assay is based on a lactate dehydrogenase cycling reaction, in which the formed NADH reduces a formazan (MTT) reagent. Exponentially grown cells (about 1×10^7 total cells) were harvested and washed three times with cold PBS. The cells were then homogenized in a 1.5 ml eppendorf tube with either 100 μl NAD extraction buffer for NAD determination or 100 μl NADH extraction buffer for NADH determination. Heated extracts at 60 °C for 5 min and then added 20 μl Assay Buffer and 100 μl of the opposite extraction buffer to neutralize the extracts. Briefly vortexed and spined the samples down at 14,000 rpm for 5 min. Use supernatant for NADH and NAD^+ assays. NADH and NAD^+ levels were measured by the microplate reader and detected at 565 nm optical density.

2.13. In vivo tumor models

Female athymic BALB/c nude mice 4–6 weeks old were purchased from the Institute of Experimental Animal of Third Military Medical University (Chongqing, China). Mice were maintained under specific

pathogen-free conditions. The mice were subcutaneously injected with HeLa cells, HeLaR cells, control cells or GLS2 silenced HeLaR cells (1×10^6 cells in 100 μl PBS/mouse) at the right hind limb. Irradiation treatment started once the xenografts were 0.6–0.8 cm in diameter. Mice were immobilized in a customized harness that exposed the right hind leg while shielding the remainder of the body behind a block of 3.5 cm thick lead. Lead shielded mice received 15 Gy of X-ray radiation by a 6MV-X linear accelerator (Varian, 23-EX) to the exposed tumor, divided into 5 fractions on days 14, 18, 22, 26, and 30. To obtain tumor growth curves, three orthogonal tumor diameters were measured at 3 day intervals with a vernier caliper, and the mean values were calculated. The animals were sacrificed (n = 5 per group) at day 34, then the xenografts were excised and weighed. Tumor volume was determined based on the following formula: volume = 0.52 ab^2, where a = long diameter and b = short diameter.

2.14. Statistical analysis

The data collected were analyzed using SPSS 13.0 software (SPSS, Chicago, IL, USA). Data points were expressed as mean ± SE of three independent experiments. Statistical significances were determined by using Student's *t*-test, Mann–Whitney *U* test or one-way ANOVA. All statistical tests were two-sided. Differences were considered statistically significant when *p*-values were less than 0.05.

3. Results

3.1. GLS2 expressions are increased in cervical cancer tissues of radioresistant patients after radiotherapy

To investigate whether the expressions of GLS2 of cervical cancers are different in patients with varying radiosensitivity, we used immunohistochemical staining to examine the expressions of GLS2 in the 58 cases of radioresistant tumor tissues, 86 cases of radiosensitive tumor tissues and 15 cases of adjacent normal tissues. The positive expressions of GLS2 in tumor tissues of radioresistant patient were much higher than those of radiosensitive patients (Fig. 1 B, C, E and F), but no positive staining had been seen in the adjacent normal cervical tissues (Fig. 1 A, D). The patient characteristics were described in Table 1. We found that the expressions of GLS2 were not correlated to the patient's age, tumor stage, tumor cell type and tumor size ($p > 0.05$) (Table 1). The results of immunohistochemical expressions of GLS2 in cervical cancer tissues (58 radioresistant and 86 radiosensitive) were summarized in Table 1. The levels of GLS2 staining were highly correlated with radiosensitivity of cervical cancer ($p < 0.05$) (Table 2).

3.2. Establishment of radioresistant HeLaR subclone cell line

We established radioresistant cell line (HeLaR) by continuously treating HeLa cells with sublethal irradiation for 6 months. To verify the radioresistant phenotypes of HeLaR, HeLaR and control HeLa cells were irradiated with a range of radiation doses (2–10 Gy) and were examined by clonogenic survival assay. Clonogenic survival assay is regarded as the gold standard for radiosensitivity [21]. As shown in Fig. 2A, HeLaR showed decreased radiosensitivity compared with control HeLa. Radiation-survival curves were derived from clonogenic survival assays of the two cell lines after different doses of X-rays (Fig. 2B). Additionally, HeLaR and HeLa were subjected to 6 Gy radiation to examine the effect on apoptosis. As shown in Fig. 2C, D, the apoptosis rate of HeLa cells was much higher than that of the radioresisitant HeLaR subline cells. Furthermore, the cell cycle distribution of HeLaR and HeLa cells after X-ray irradiation was determined by flow cytometry. As shown in Fig. 2E, F, 24 h after 6 Gy irradiation, HeLaR cells were found detained more cells in S phase with less cells in G2-M phase compared with HeLa cells, suggesting that the regulation of cell cycle induced by ionizing radiation is altered in the radioresistant HeLaR, which is also consistent with the typical radioresistant phenotype. All these results indicate that the sub-line HeLaR is more radioresistant than the parental HeLa cell line.

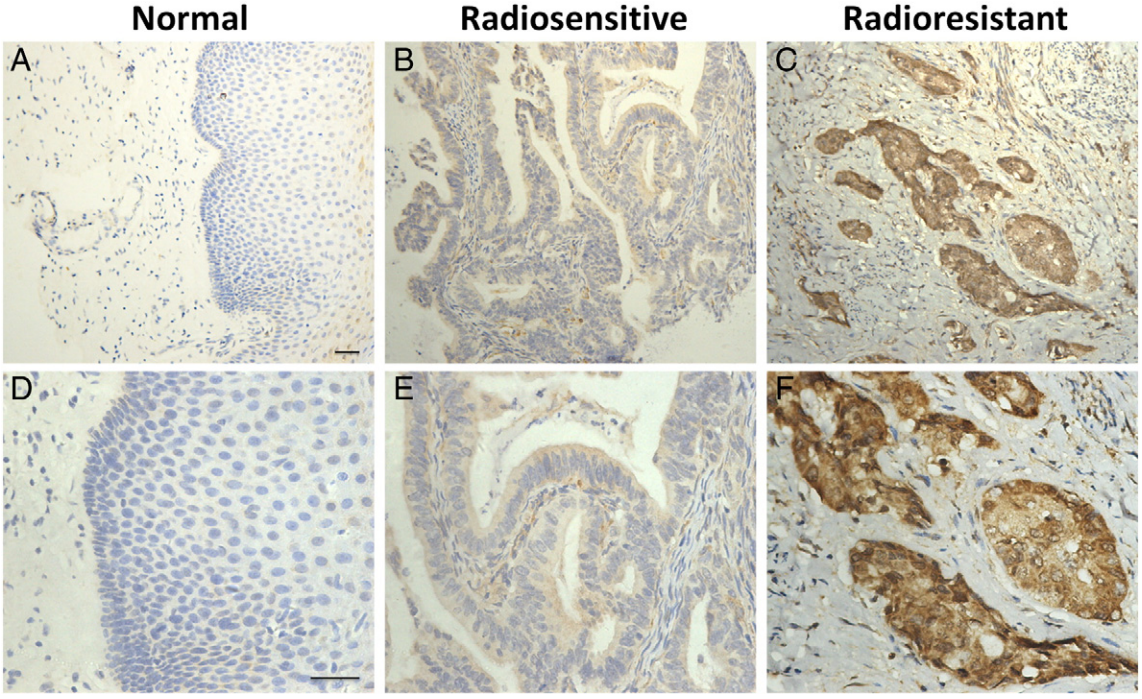

Fig. 1. Expressions of endogenous GLS2 in human cervical cancer tissues of radioresistant patients and radiosensitive patients. The immunohistochemistry staining of GLS2 in adjacent normal cervical tissues (A), cervical cancer tissues of radiosensitive patients (B) and radioresistant patients (C). The bottom panel shows higher magnification of GLS2 staining in adjacent normal cervical tissues (D), cervical cancer tissues of radiosensitive patients (E) and radioresistant patients (F). Scale bar = 50 μm.

Table 1
Patient characteristics.

Characteristics	Radiation-resistant (n = 86)	Radiation-sensitive (n = 58)	*p*-Value
Age(mean)	60	61	>0.05
<50	33	21	
≥50	53	37	
Stage			>0.05
IIB	17	14	
IIIA	31	11	
IIIB	29	23	
IVA	9	10	
Cell type			>0.05
Squamous carcinoma	68	47	
Adenocarcinoma	18	11	
Size(cm)			>0.05
<4.0 cm	55	39	
≥4.0 cm	31	19	
Primary treatment			
RT	81	55	
CCRT	5[a]	3[b]	

RT: radiation therapy, CCRT: concurrent chemoradiation therapy.
[a] Cisplatin + 5FU.
[b] Cisplatin + 5FU (n = 2) and weekly Cisplatin (n = 1).

3.3. Knocking down of GLS2 reverses radioresistance of cervical cancer cells in vitro

We measured the GLS2 levels in different cancer cell lines HepG2, HT29, A549, CE109, MCF-7, SGC7901, HeLa and SW620, and had verified that GLS2 were only expressed in MCF-7 and HeLa cells (Fig. 3A). We further detected the expressions of GLS2 in radioresistant HeLaR cells together with their wild type cells. We found that the expressions of GLS2 were much higher in HeLaR than that in HeLa (Fig. 3B). To determine if GLS2 is critical in affecting radioresistance of cervical cancer, we generated lentivector expressing GLS2-specific short hairpin RNA (shRNA) that could efficiently silence the expressions of GLS2 in transfected HeLaR cells (Fig. 3B). Then, clonogenic survival assay was performed to measure the radiation response. As shown in Fig. 3C, D, GLS2 knockdown cells displayed weaker colony formation capacity compared to other control groups. Intriguingly, the colony formation capacity of HeLa cells was intermediate between HeLaR cells and GLS2 knockdown cells. We further measured the cellular apoptosis in different groups under irradiation. It showed that more apoptotic cells were detected in GLS2 knockdown group than radioresistant or control group at 48 h after 6 Gy irradiation (Fig. 3E). The above results indicate that knocking down the expressions of GLS2 can dramatically increase the radiosensitivity of HeLaR cells.

3.4. Knocking down GLS2 alters intracellular ROS via decreasing glutathione, NADH and NADPH levels

Intracellular ROS levels can affect the sensitivity of cells to ionizing radiation-induced apoptosis. We hypothesized that decreasing GLS2 expression would lead to elevated levels of intracellular ROS. To address this hypothesis, the oxidizable fluorogenic probe DHE was used to examine the redox levels of GLS2 knockdown HeLaR cells, HeLaR cells and wild type HeLa cells. As shown in Fig. 4B, reduced GLS2 expressions led to a vast increase in ROS levels in both unstressed and ionizing radiation-treated cells by flow cytometry. Notably, these GLS2-negative cells displayed approximately 2.5-fold higher ROS levels compared with HeLaR cells after 6 Gy irradiation (Fig. 4B). Immunofluorescence staining was further employed to detect the intracellular ROS levels. Down-regulation of GLS2 resulted in increased oxidation of DHE (blue) to 2-OH-E^+ (red) when compared to HeLaR and control cells (Fig. 4A). This data was consistent with the intracellular ROS levels seen in the quantitative analysis by flow cytometry (Fig. 4B). GLS2 regulates one of the precursors of GSH, the most important antioxidant molecule and a scavenger for ROS, and GSH/oxidized glutathione (GSSG) is the major redox couple that determines the antioxidative capacity of cells [22]. We measured the GSH levels and GSH/GSSG ratio in different groups. Our results showed that HeLaR cells displayed higher levels of GSH and GSH/GSSG ratio compared with other groups, whereas knocking down of GLS2 expression decreased GSH levels and the GSH/GSSG ratio in cells (Fig. 4C, D). Given that NADH and NADPH are also important intracellular antioxidants, we further detected NAD^+/NADH ratio as well as $NADH^+$/NADPH ratio in different groups. Consistent with previous findings, silencing GLS2 significantly decreased NADH and NADPH levels in cells (Fig. 4E and F). Taken together, these data indicate that GLS2 regulates intracellular ROS levels through the GSH, NADH and NADPH-dependent antioxidant systems.

Table 2
Immunohistochemical analysis of GLS2 expression in radiation-sensitive and radiation-resistant cervical cancer tissues.

	GLS2 staining				Total (n = 144)	*p*-Value
	0 ~ 3	4 ~ 6	7 ~ 9	10 ~ 12		
Radiation-sensitive	20	33	21	12	86	0.000257
Radiation-resistant	6	12	27	13	58	

3.5. Knocking down GLS2 expression enhances the radiosensitivity of cervical cancer xenografts

Mouse xenograft models were established to determine whether knocking down of GLS2 confers a sensitive phenotype of radioresistant cervical cancer to radiation *in vivo*. The groups consisted of the following (5 mice for each group): wide type HeLa group, radioresistant HeLaR group, empty vector lentiviruses transfected HeLaR group (control shRNA) and GLS2-shRNA lentiviruses transfected HeLaR group (shRNA-GLS2). All animals received 15 Gy of X-ray radiation divided into 5 fractions when the xenografts in each group reached a mean diameter of 0.6–0.8 cm. At the end of the experiment, the animals were sacrificed and the xenografts were removed. The tumor volumes were determined and presented as a fold increase or decrease compared to the tumor size at the primary site (day 12) of each group. By day 25, the tumor size of HeLaR and control shRNA groups was approximately 4.5-fold greater than that at day 12 respectively, whereas the tumor size of shRNA-GLS2 group was only about 2-fold greater than the initial tumor size at day 12 (Fig. 5B). After that, a significant delay in tumor growth was observed. As shown in Fig. 5A and B, the size of the xenografts in GLS2 knockdown group decreased more dramatically than those in radioresistant group and other groups. Additionally, xenografts were weighed when the mice were sacrificed at the end of the experiment. As shown in Fig. 5C, the weight of GLS2 knockdown tumors was dramatically reduced compared to other groups in response to radiation.

4. Discussion

It is widely known that the first reaction in glutamine metabolism is hydrolysis of glutamine to glutamate *via* the amidohydrolase enzyme glutaminase. Humans express two major isoforms of this enzyme: GLS1 (kidney-type) and GLS2 (liver-type) from two closely related genes [23]. It has also been reported that GLS1 and GLS2 seem to have contrasting effects in tumorigenesis [10]. GLS1 is abundantly expressed in transformed and rapidly dividing cells. Thus, it has been considered as "tumor type" because of its function in promoting oncogenic transformation and proliferation of different types of tumors [24]. While, GLS2 is most likely to be absent in a majority of malignant tumors [25].

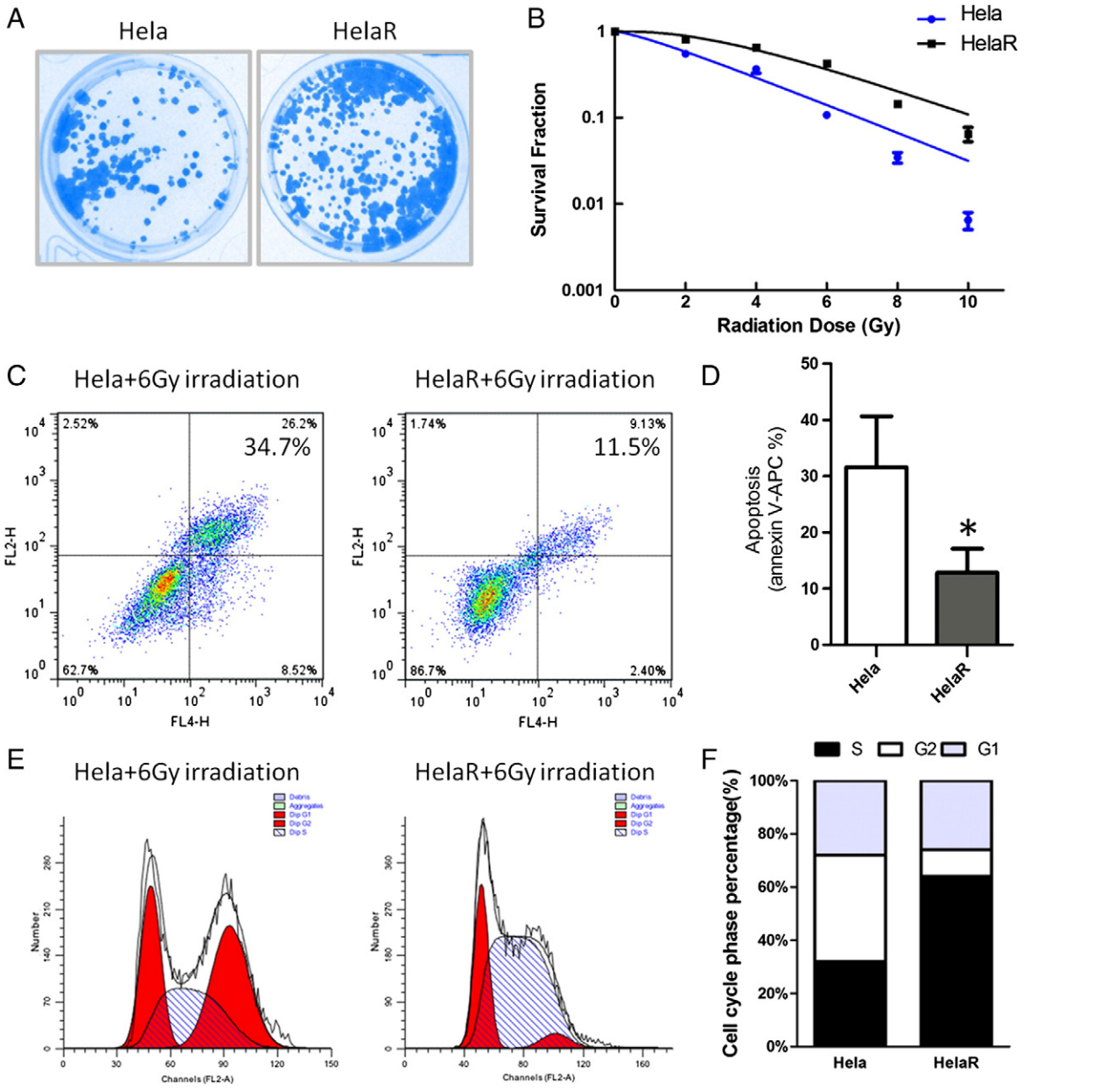

Fig. 2. Different radiation-sensitivity of X-ray resistant sub-line HeLaR and the parental HeLa cells. (A) Images of the colonies formed from HeLaR and HeLa cells at 48 h after 6 Gy irradiation. (B) Dose-survival fraction curves of HeLaR and HeLa cells in the presence of different dose of radiation (0–10 Gy). (C, D) Apoptosis assay of HeLaR and HeLa cells at 48 h after 6 Gy irradiation (*$p < 0.05$). The error bars are the mean ± SE. (E, F) Cell cycle distribution of HeLaR and HeLa cells at 24 h after 6 Gy irradiation. The results shown are the average of three independent experiments.

Although GLS2 was originally thought to be present mostly in normal tissue [12], emerging evidence has revealed that GLS2 expression also occurs in malignant tumor cells, for example, breast cancer cells [13]. Furthermore, our present finding demonstrated that GLS2 is also expressed in cervical cancer. We wondered, to a certain extent, that GLS2 should be considered as the "tumor type" at least in breast cancer and cervical cancer. More significantly, the major finding of this study was that GLS2 is required for maintaining radioresistance of cervical cancer. To our knowledge, this study is for the first to link GLS2 to radiosensitivity of cervical cancer cells.

It is interesting to find that advance staged human cervical cancer showed higher levels of GLS2 in radioresistant patient group than radiosensitive patient group. One plausible speculation is that GLS2 may play an important role in mediating radioresistance of cervical cancer. To address this hypothesis, we established a stable radioresistant human cervical cancer cell line and investigated the biochemical pathways involved in GLS2-enhanced cell radioresistance. Our data demonstrate that the expression of GLS2 is also higher in radioresistant cancer cells than radiosensitive cells. This finding is consistent with the clinical observation that failure of radiotherapy in cervical cancers is usually associated with enhanced levels of GLS2. Then, we used shRNA to stably knock down GLS2 expression in radioresistant cervical cancer cell line. We found that knocking down GLS2 significantly enhanced radiosensitivity of cervical cancer cells *in vitro* and *in vivo*. Furthermore, our studies have shed light on the underlying mechanism through which GLS2 mediating radioresistance of cervical cancer.

Radiotherapy is based on the fact that ionizing radiation destroys tumor cells. A primary mechanism of ionizing radiation against cancer cells is the formation of reactive oxygen species (ROS), or free radicals [26]. When H_2O, the most abundant intracellular molecule, is exposed

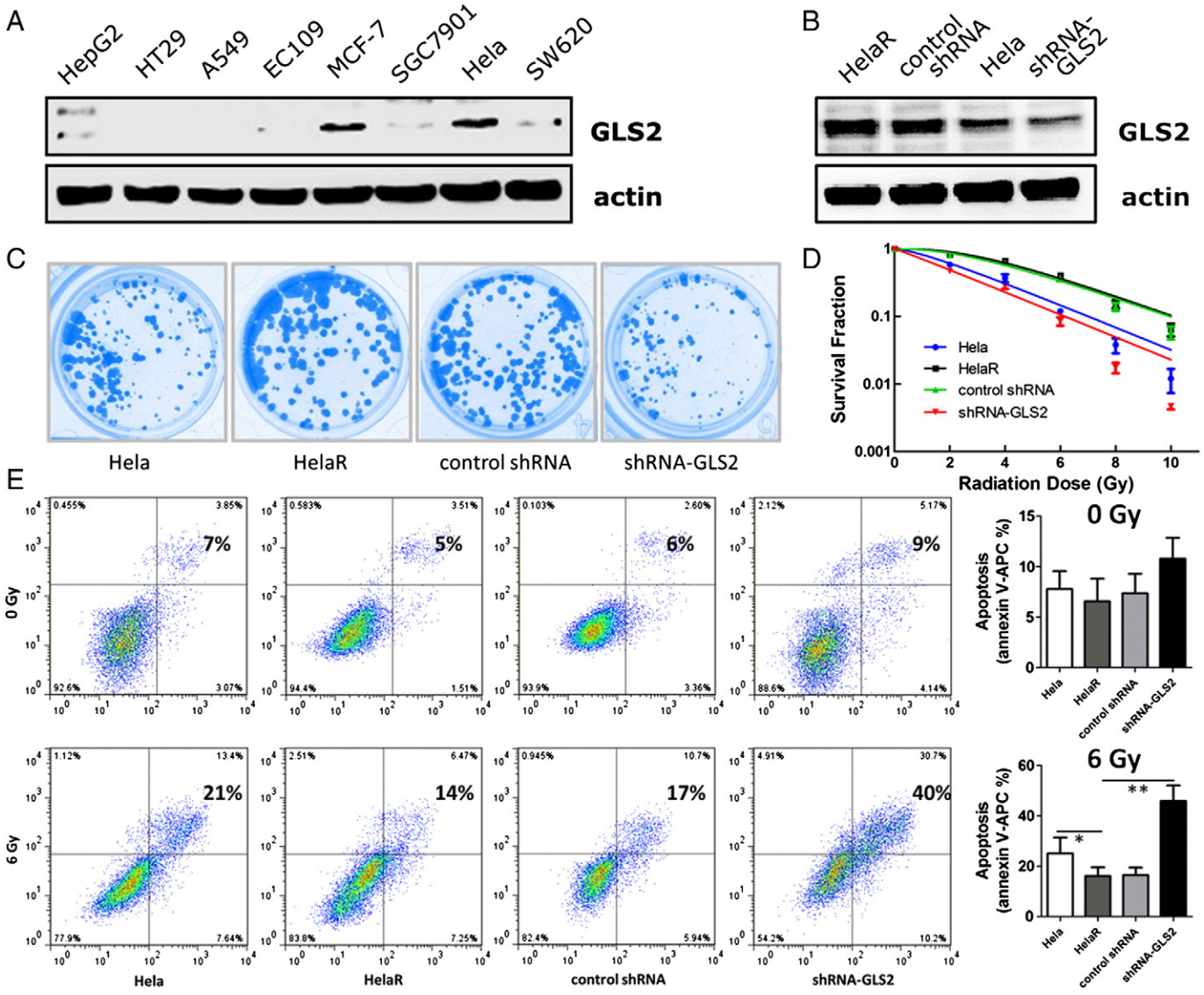

Fig. 3. The effect of GLS2 knockdown on radiosensitivity of cervical cancer cells *in vitro*. (A) The protein levels of GLS2 in different cancer cell lines. (B) The protein levels of GLS2 in HeLa cells, HeLaR cells and HeLaR cells that were stably infected with GLS2-shRNA lentiviruses (shRNA-GLS2) or empty vector lentiviruses (control shRNA). (C) Images of the colonies formed from HeLa, HeLaR, control shRNA and shRNA-GLS2 cells in the presence of irradiation. (D) Dose-survival fraction curves of HeLa, HeLaR, control shRNA and shRNA-GLS2 cells in the presence of different dose of radiation (0–10 Gy) respectively. (E) Apoptosis assay of HeLa, HeLaR, control shRNA and shRNA-GLS2 cells at 48 h after 0 Gy and 6 Gy irradiation ($^{*}p < 0.05$, $^{**}p < 0.01$). Data are mean ± SE, n = 3.

to ionizing radiation, decomposition reactions occur, which generate a variety of free radicals such as superoxide anion radical ($O_2^{\bullet -}$), hydrogen peroxide (H_2O_2) and hydroxyl radical (•OH). Excessive accumulation of ROS within cells results in oxidative stress that leads to oxidative damage to critical cellular biomolecules (DNA, protein, and lipids) [27]. In a word, ROS plays a critical role in cell death caused by ionizing radiation [28]. However, ionizing radiation-induced changes in cellular antioxidant defense system are believed to suppress ROS-induced cytotoxicity [29]. Glutathione (GSH), one of the major antioxidant enzymes is known to play an important role in cellular defense against radiation [26]. GSH not only directly scavenges ROS, reactive nitrogen species, and reactive metabolites but also serves as an important cofactor in enzymatic redox reactions [30,31]. Several previous studies indicated that chemo- and radio-resistant tumor cells have increased GSH levels [32]. Depletion of GSH caused enhancement of radiosensitivity in different human tumor cells [33,34]. GLS2 regulates cellular production of glutamate which is one of the precursors of GSH [10]. We wondered whether GSH contributes to the GLS2-enhanced radioresistance of cervical cancer. To address this question, we detected the levels of GSH in GLS2 knockdown cells. Interestingly, GLS2 knockdown decreased GSH levels and the GSH/GSSG ratio, whereas there is a significantly increasing of GSH levels and the GSH/GSSG ratio in radioresistant tumor cells. Our findings are consistent with results from other researchers, who also showed that GLS2 could increase GSH production and decrease ROS levels in cells [35].

Altering the expression of one antioxidant enzyme may influence the expression of other antioxidant enzymes as compensatory mechanisms in order to sustain a reduced redox environment [26]. NADH and NADPH are also known as important intracellular antioxidants and reductants. Our results further showed that GLS2 expression regulates intracellular NADH and NADPH production. We found that NADH and NADPH levels also enhanced in radioresistant tumor cells, whereas GLS2 knockdown decreased NADH and NADPH levels in resistant cervical cancer cells. Taken together, we have shown that GLS2 plays an important role in regulating radiosensitivity of human cervical carcinomas. Decreasing GLS2 expression in radioresistant cervical cancer cells

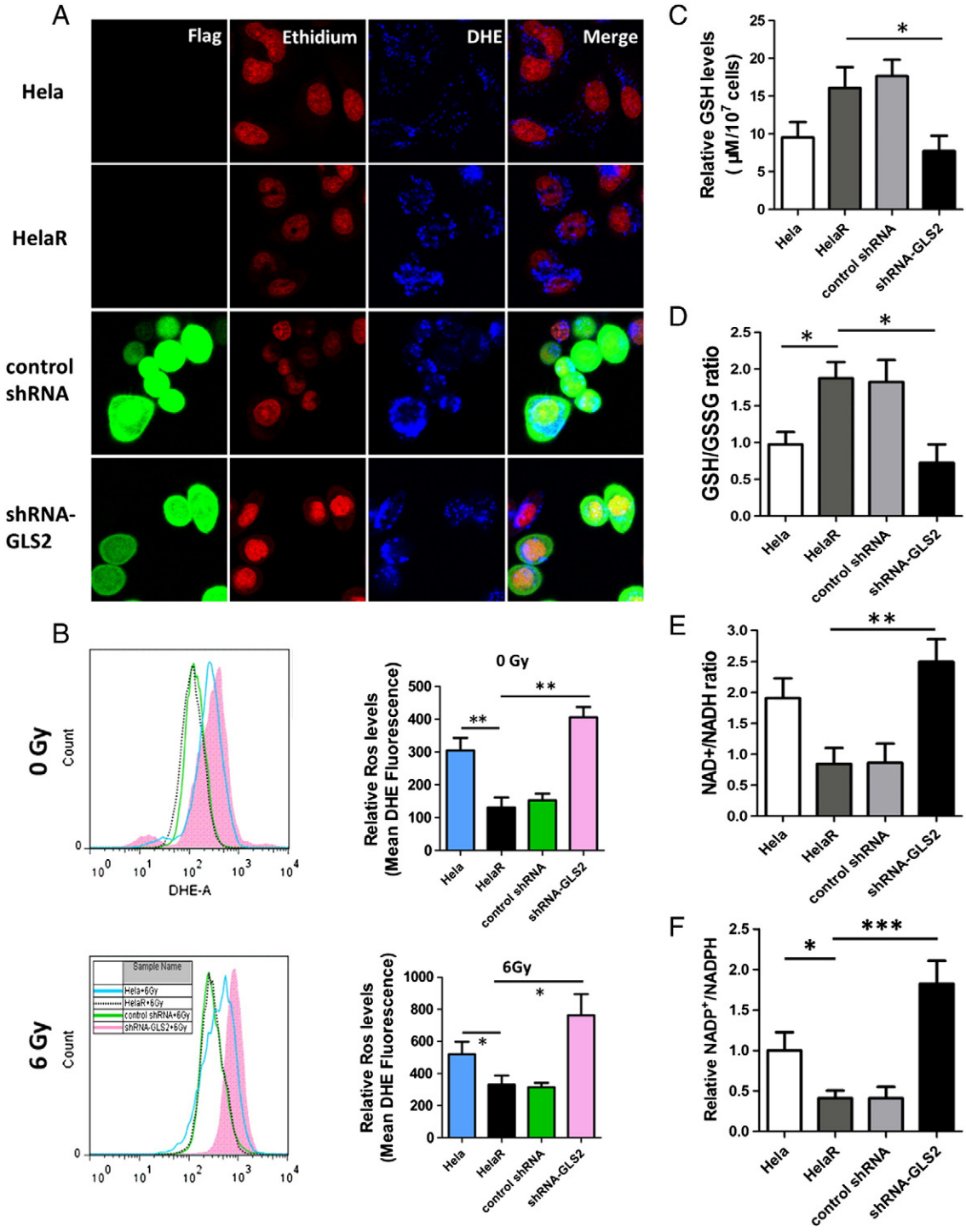

Fig. 4. The effect of GLS2 knockdown on changing intracellular ROS levels response to irradiation and controlling intracellular antioxidants. (A) Representative confocal images of intracellular ROS (red) produced by HeLa, HeLaR, control shRNA and shRNA-GLS2 cells in the presence of irradiation. (B) Flow cytometry measurement of fluorescence intensity of intracellular ROS from different groups in the presence of 0 Gy and 6 Gy irradiation respectively. Detection of intracellular GSH levels (C), relative GSH/GSSG ratio (D), relative NAD^+/NADH ratio (E) and relative $NADH^+$/NADPH ratio (F). (mean ± SE; n = 3; $^*p < 0.05$, $^{**}p < 0.01$, $^{***}p < 0.001$).

increases *in vitro* and *in vivo* sensitivity to ionizing radiation. In addition, our data indicate that downregulation of GLS2 expression decreases cellular antioxidants GSH, NADH and NADPH production and eventually increases cellular ROS levels, which suggests a possible mechanism for the observed sensitization.

Regarding to the molecular mechanism which leading to the GLS2 overexpression in cervical cancer, we are thinking that GLS2 might be induced by activation of radiation dependent EGFR/ERK signaling pathway. As we know cells respond to irradiation damage by triggering the activation of cell surface receptors, such as epidermal growth factor receptor (EGFR)[36], resulting in the phosphorylation of extracellular signal-regulated kinase (ERK), p38 MAPK (p38 kinase), or c-Jun NH2-terminal kinases (JNK) signaling pathways[37,38]. We found that phosphorylation of ERK is increased in HeLaR cells but not MAPK or JNK (data not shown). Additionally, recent data from other labs show that activated ERK signaling pathway upregulates glutamine metabolism as well as glutaminase activity [39,40]. Our further work is to confirm whether EGFR/ERK signaling pathway upregulates GLS2 expression in

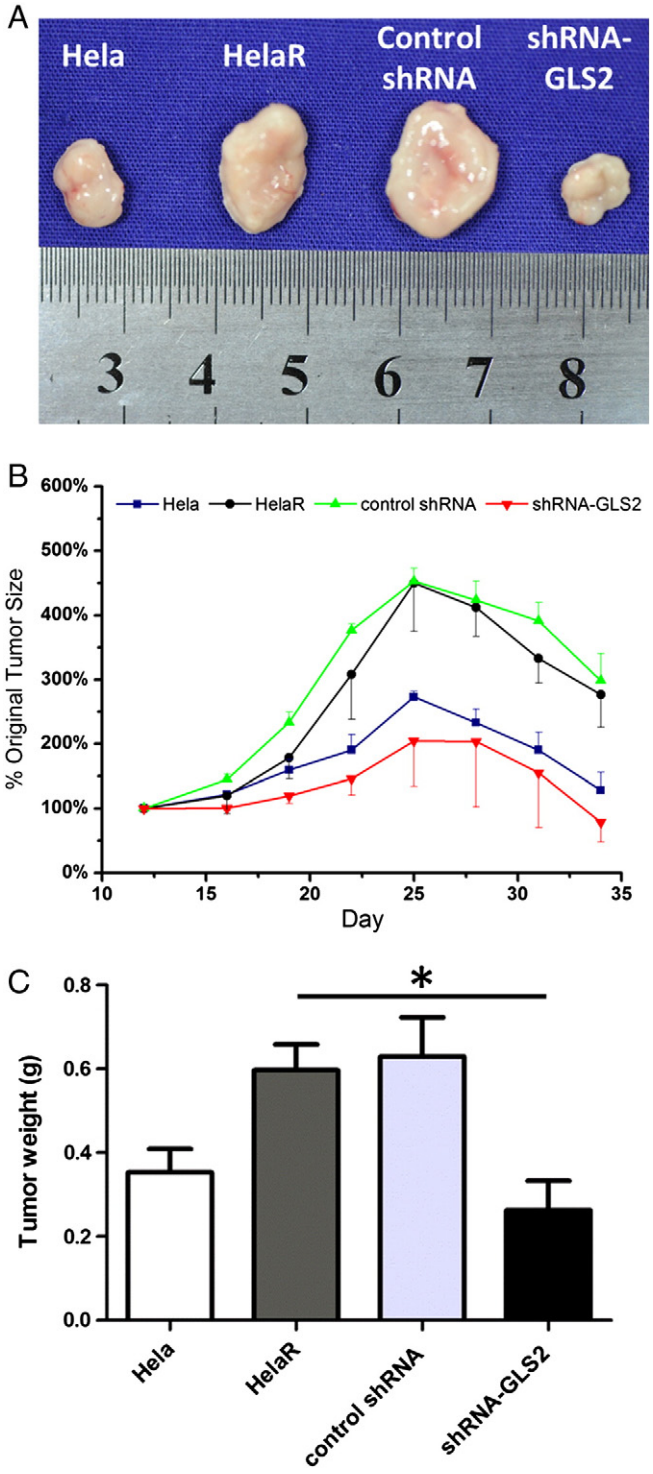

Fig. 5. The effect of GLS2 knockdown on radiosensitivity of cervical cancer cells in xenografts. (A) The final tumor volumes in different tumor groups after irradiation treatment. Animals (n = 5 per group) received 15 Gy of X-radiation divided into 5 fractions on days 14, 18, 22, 26, and 30. (B) The growth curves of xenografts generated by HeLa, HeLaR, control shRNA and shRNA-GLS2 cells. Data are expressed as the mean change in tumor volumes relative to the initial tumor volumes on day 12. (C) The statistical histogram of the final xenografts weight in different groups of sacrificed mice is also shown (*$p < 0.05$).

radioresistant cervical cancer cells. Furthermore, we speculate that some transcriptional factors might also contribute to the upregulation of GLS2, such as hypoxia inducible factor-1 (HIF-1). Hypoxia and HIF-1 are significantly associated with cancer resistance to radiotherapy. There are increased data show that hypoxia regulate the activity levels of glutamine synthetase, glutaminase as well as glutamate metabolism [41,42]. We also try to find out whether HIF-1 could regulate GLS2 expression in a directly or indirectly way.

Given the role of GLS2 in mediating cervical cancer radioresistance, GLS2 should be a potential target to improve the efficiency of radiosensitivity in cervical cancer. Future investigations should be focus on the role of some other intracellular antioxidants which may also involve in GLS2-mediating radioresistance of cervical cancer. Additionally, precise mechanisms responsible for the GLS2 signaling pathway are required.

Conflict of interest statement

The authors declare that they have no conflict of interest.

Acknowledgements

Grant support: This work was funded by the National Natural Science Foundation of China (No. 81301841, No. 81172115 and No. 81272364), and the Preclinical Medicine Project of the Third Military Medical University (No. 2012XJQ14).

References

[1] J. Ponten, H.O. Adami, R. Bergstrom, J. Dillner, L.G. Friberg, L. Gustafsson, A.B. Miller, D.M. Parkin, P. Sparen, D. Trichopoulos, Strategies for global control of cervical cancer, Int. J. Cancer 60 (1995) 1–26.
[2] J. Ferlay, H.R. Shin, F. Bray, D. Forman, C. Mathers, D.M. Parkin, Estimates of worldwide burden of cancer in 2008: GLOBOCAN 2008, Int. J. Cancer 127 (2010) 2893–2917.
[3] P. Petignat, M. Roy, Diagnosis and management of cervical cancer, BMJ 335 (2007) 765–768.
[4] J.F. Ward, Mechanisms of DNA repair and their potential modification for radiotherapy, Int. J. Radiat. Oncol. Biol. Phys. 12 (1986) 1027–1032.
[5] L.B. Harrison, M. Chadha, R.J. Hill, K. Hu, D. Shasha, Impact of tumor hypoxia and anemia on radiation therapy outcomes, Oncologist 7 (2002) 492–508.
[6] A. Taghian, H. Suit, F. Pardo, D. Gioioso, K. Tomkinson, W. DuBois, L. Gerweck, In vitro intrinsic radiation sensitivity of glioblastoma multiforme, Int. J. Radiat. Oncol. Biol. Phys. 23 (1992) 55–62.
[7] M. Miura, T. Sasaki, Role of glutathione in the intrinsic radioresistance of cell lines from a mouse squamous cell carcinoma, Radiat. Res. 126 (1991) 229–236.
[8] J. Blickwedehl, S. Olejniczak, R. Cummings, N. Sarvaiya, A. Mantilla, A. Chanan-Khan, T.K. Pandita, M. Schmidt, C.B. Thompson, N. Bangia, The proteasome activator PA200 regulates tumor cell responsiveness to glutamine and resistance to ionizing radiation, Mol. Cancer Res. 10 (2012) 937–944.
[9] W.W. Souba, V.S. Klimberg, E.M. Copeland III, Glutamine nutrition in the management of radiation enteritis, JPEN J. Parenter. Enteral Nutr. 14 (1990) 106S–108S.
[10] J.M. Mates, J.A. Segura, M. Martin-Rufian, J.A. Campos-Sandoval, F.J. Alonso, J. Marquez, Glutaminase isoenzymes as key regulators in metabolic and oxidative stress against cancer, Curr. Mol. Med. 13 (2013) 514–534.
[11] N.P. Curthoys, M. Watford, Regulation of glutaminase activity and glutamine metabolism, Annu. Rev. Nutr. 15 (1995) 133–159.
[12] M. Watford, Hepatic glutaminase expression: relationship to kidney-type glutaminase and to the urea cycle, FASEB J. 7 (1993) 1468–1474.
[13] P.M. Gomez-Fabre, J.C. Aledo, A. Del Castillo-Olivares, F.J. Alonso, I. Nunez De Castro, J.A. Campos, J. Marquez, Molecular cloning, sequencing and expression studies of the human breast cancer cell glutaminase, Biochem. J. 345 (Pt 2) (2000) 365–375.
[14] J. Marquez, A.R. de la Oliva, J.M. Mates, J.A. Segura, F.J. Alonso, Glutaminase: a multifaceted protein not only involved in generating glutamate, Neurochem. Int. 48 (2006) 465–471.
[15] J.B. Wang, J.W. Erickson, R. Fuji, S. Ramachandran, P. Gao, R. Dinavahi, K.F. Wilson, A.L. Ambrosio, S.M. Dias, C.V. Dang, R.A. Cerione, Targeting mitochondrial glutaminase activity inhibits oncogenic transformation, Cancer Cell 18 (2010) 207–219.
[16] L.M. Shelton, L.C. Huysentruyt, T.N. Seyfried, Glutamine targeting inhibits systemic metastasis in the VM-M3 murine tumor model, Int. J. Cancer 127 (2010) 2478–2485.
[17] B.C. Fuchs, R.E. Finger, M.C. Onan, B.P. Bode, ASCT2 silencing regulates mammalian target-of-rapamycin growth and survival signaling in human hepatoma cells, Am. J. Physiol. Cell Physiol. 293 (2007) C55–C63.
[18] P. Nicklin, P. Bergman, B. Zhang, E. Triantafellow, H. Wang, B. Nyfeler, H. Yang, M. Hild, C. Kung, C. Wilson, V.E. Myer, J.P. MacKeigan, J.A. Porter, Y.K. Wang, L.C. Cantley, P.M. Finan, L.O. Murphy, Bidirectional transport of amino acids regulates mTOR and autophagy, Cell 136 (2009) 521–534.
[19] G.J. Duan, X.C. Yan, X.W. Bian, J. Li, X. Chen, The significance of beta-catenin and matrix metalloproteinase-7 expression in colorectal adenoma and carcinoma, Zhonghua Bing Li Xue Za Zhi 33 (2004) 518–522.
[20] M.A. Baker, G.J. Cerniglia, A. Zaman, Microtiter plate assay for the measurement of glutathione and glutathione disulfide in large numbers of biological samples, Anal. Biochem. 190 (1990) 360–365.

[21] A. Yaromina, M. Krause, H. Thames, A. Rosner, M. Krause, F. Hessel, R. Grenman, D. Zips, M. Baumann, Pre-treatment number of clonogenic cells and their radiosensitivity are major determinants of local tumour control after fractionated irradiation, Radiother. Oncol. 83 (2007) 304–310.
[22] H. Sies, Glutathione and its role in cellular functions, Free Radic. Biol. Med. 27 (1999) 916–921.
[23] J.C. Aledo, P.M. Gomez-Fabre, L. Olalla, J. Marquez, Identification of two human glutaminase loci and tissue-specific expression of the two related genes, Mamm. Genome 11 (2000) 1107–1110.
[24] C. Lobo, M.A. Ruiz-Bellido, J.C. Aledo, J. Marquez, I. Nunez De Castro, F.J. Alonso, Inhibition of glutaminase expression by antisense mRNA decreases growth and tumourigenicity of tumour cells, Biochem. J. 348 (Pt 2) (2000) 257–261.
[25] M. Szeliga, M. Obara-Michlewska, E. Matyja, M. Lazarczyk, C. Lobo, W. Hilgier, F.J. Alonso, J. Marquez, J. Albrecht, Transfection with liver-type glutaminase cDNA alters gene expression and reduces survival, migration and proliferation of T98G glioma cells, Glia 57 (2009) 1014–1023.
[26] J.M. Mates, J.A. Segura, F.J. Alonso, J. Marquez, Oxidative stress in apoptosis and cancer: an update, Arch. Toxicol. 86 (2012) 1649–1665.
[27] J.E. Biaglow, J.B. Mitchell, K. Held, The importance of peroxide and superoxide in the X-ray response, Int. J. Radiat. Oncol. Biol. Phys. 22 (1992) 665–669.
[28] A. Morales, M. Miranda, A. Sanchez-Reyes, A. Biete, J.C. Fernandez-Checa, Oxidative damage of mitochondrial and nuclear DNA induced by ionizing radiation in human hepatoblastoma cells, Int. J. Radiat. Oncol. Biol. Phys. 42 (1998) 191–203.
[29] G. Guo, Y. Yan-Sanders, B.D. Lyn-Cook, T. Wang, D. Tamae, J. Ogi, A. Khaletskiy, Z. Li, C. Weydert, J.A. Longmate, T.T. Huang, D.R. Spitz, L.W. Oberley, J.J. Li, Manganese superoxide dismutase-mediated gene expression in radiation-induced adaptive responses, Mol. Cell. Biol. 23 (2003) 2362–2378.
[30] F.Q. Schafer, G.R. Buettner, Redox environment of the cell as viewed through the redox state of the glutathione disulfide/glutathione couple, Free Radic. Biol. Med. 30 (2001) 1191–1212.
[31] D.M. Townsend, K.D. Tew, H. Tapiero, The importance of glutathione in human disease, Biomed. Pharmacother. 57 (2003) 145–155.
[32] J.M. Estrela, A. Ortega, E. Obrador, Glutathione in cancer biology and therapy, Crit. Rev. Clin. Lab. Sci. 43 (2006) 143–181.
[33] J.E. Biaglow, M.E. Varnes, S.W. Tuttle, N.L. Oleinick, K. Glazier, E.P. Clark, E.R. Epp, L.A. Dethlefsen, The effect of L-buthionine sulfoximine on the aerobic radiation response of A549 human lung carcinoma cells, Int. J. Radiat. Oncol. Biol. Phys. 12 (1986) 1139–1142.
[34] E.P. Clark, Thiol-induced biochemical modification of chemo- and radio responses, Int. J. Radiat. Oncol. Biol. Phys. 12 (1986) 1121–1126.
[35] W. Hu, C. Zhang, R. Wu, Y. Sun, A. Levine, Z. Feng, Glutaminase 2, a novel p53 target gene regulating energy metabolism and antioxidant function, Proc. Natl. Acad. Sci. U. S. A. 107 (2010) 7455–7460.
[36] C. Sachsenmaier, A. Radler-Pohl, R. Zinck, A. Nordheim, P. Herrlich, H.J. Rahmsdorf, Involvement of growth factor receptors in the mammalian UVC response, Cell 78 (1994) 963–972.
[37] L. Jinlian, Z. Yingbin, W. Chunbo, p38 MAPK in regulating cellular responses to ultraviolet radiation, J. Biomed. Sci. 14 (2007) 303–312.
[38] C. Lopez-Camarillo, E.A. Ocampo, M.L. Casamichana, C. Perez-Plasencia, E. Alvarez-Sanchez, L.A. Marchat, Protein kinases and transcription factors activation in response to UV-radiation of skin: implications for carcinogenesis, Int. J. Mol. Sci. 13 (2012) 142–172.
[39] E.L. Carr, A. Kelman, G.S. Wu, R. Gopaul, E. Senkevitch, A. Aghvanyan, A.M. Turay, K.A. Frauwirth, Glutamine uptake and metabolism are coordinately regulated by ERK/MAPK during T lymphocyte activation, J. Immunol. 185 (2010) 1037–1044.
[40] K. Thangavelu, C.Q. Pan, T. Karlberg, G. Balaji, M. Uttamchandani, V. Suresh, H. Schuler, B.C. Low, J. Sivaraman, Structural basis for the allosteric inhibitory mechanism of human kidney-type glutaminase (KGA) and its regulation by Raf-Mek-Erk signaling in cancer cell metabolism, Proc. Natl. Acad. Sci. U. S. A. 109 (2012) 7705–7710.
[41] P. Vats, A.K. Mukherjee, M.M. Kumria, S.N. Singh, S.K. Patil, S. Rangnathan, K. Sridharan, Changes in the activity levels of glutamine synthetase, glutaminase and glycogen synthetase in rats subjected to hypoxic stress, Int. J. Biometeorol. 42 (1999) 205–209.
[42] S. Kobayashi, D.E. Millhorn, Hypoxia regulates glutamate metabolism and membrane transport in rat PC12 cells, J. Neurochem. 76 (2001) 1935–1948.